Available online at www.sciencedirect.com

ScienceDirect

Procedia Computer Science 49 (2015) 332 – 339

Procedia Computer Science

ICAC3'15

Artificial Neural Network Model for Suspended Rectangular Microstrip Antennas

Amit A. Deshmukh[1], Shivali D. Kulkarni[2], Venkata A.P.C.[1], Neelam V. Phatak[1]

1. EXTC, DJSCOE, Vile – Parle (W), Mumbai, India
2. ELEX, DJSCOE, Vile – Parle (W), Mumbai, India
Email – amitdeshmukh76@rediffmail.com

Abstract

The broadband microstrip antenna is more commonly realized by fabricating the patch on lower dielectric constant thicker substrate. While using thicker substrate, close form expressions for calculating edge extension length due to fringing fields is not available. In this paper, an artificial neural network model for suspended rectangular microstrip antenna is proposed. The resonance frequency calculated by using the proposed neural network model closely agrees with simulated and measured results over wide frequency range and for varying thicker substrates. Thus the proposed model can be used to accurately calculate the side length of rectangular microstrip antenna.

Peer-review under responsibility of organizing committee of the 4th International Conference on Advances in Computing, Communication and Control (ICAC3'15)

Keywords: Rectangular Microstrip antenna, Suspended microstrip antenna, Artificial Neural Network model, Thicker substrate;

1. Introduction

The broadband microstrip antenna (MSA) is realized by fabricating the patch on lower dielectric constant thicker substrate [1 – 3]. In most of the reported literature, the patch is suspended in air thereby realizing dielectric constant of unity. The radiating patch in MSA can take any arbitrary shapes but more commonly regular radiating patch geometries like rectangular, circular, equilateral triangular, elliptical and isosceles have

Peer-review under responsibility of organizing committee of the 4th International Conference on Advances in Computing, Communication and Control (ICAC3'15)
doi:10.1016/j.procs.2015.04.261

been used. In most of these patch geometries, while designing them on thinner substrates ($h \leq 0.03\lambda_0$), resonance frequency formulation is available [1 – 3]. While calculating resonance frequency, effective patch dimensions is needed to be considered, this accounts for fringing field extension present towards patch periphery. Depending upon the operating mode, for calculating resonance frequency in rectangular MSA (RMSA), an edge extension length is added to patch length or width. The expressions for them are available for thinner substrates. However they are not available while using thicker substrates and at different resonance frequencies. Therefore for designing broadband MSAs on thicker substrate ($h > 0.06\lambda_0$) patch dimensions cannot be accurately calculated. The artificial neural network (ANN) model for RMSA is reported, but they do not calculate patch dimensions over wide range of frequencies and substrate thickness [4, 5].

In this paper, ANN model for predicting the resonance frequency of RMSA at its fundamental TM_{10} mode is proposed. The ANN model is proposed for varying substrate thickness and over wide frequency range from 500 to 6000 MHz. At all the frequencies, while predicting resonance frequency (patch length) using ANN model, substrate thickness for RMSA is taken to be less than $0.1\ \lambda_0$. Since in most of the reported broadband RMSA configurations, an air substrate is used (as it helps in realizing larger gain and bandwidth), the same is used while developing ANN model. In the proposed work, first using resonance frequency equation for RMSA, and further by simulating the same using IE3D software, an edge extension length for different substrate thickness and over wide frequency range is calculated [6]. Further, parameters like, substrate thickness, fringing field extension length, dielectric constant at different resonance frequencies is given as input to the neural network model. Using the developed neural network model, patch side length at different resonance frequencies and for different substrate thickness is predicted. For realizing optimum gain, patch width is taken to be 1.2 times the patch length. The RMSA for predicted dimensions is further simulated using IE3D software. It is observed that the simulated frequency shows closer agreement with the predicted neural network value. Further to verify the predicted and simulated results, measurements were carried out. They show closer agreement with simulated and measured result. Similar ANN model is developed for suspended RMSA in which radiating patch is fabricated on glass epoxy substrate ($\varepsilon_r = 4.3$, $h_e = 0.16$ cm, $\tan\delta = 0.02$) which is suspended above the ground plane with an air gap 'Δ'. The model for suspended RMSA also shows closer agreement between simulated, measured and predicted values. Thus the proposed model can be used to accurately calculate the patch dimension in RMSA for given substrate thickness and frequency.

2. SUSPENDED RMSA

The coaxially fed RMSA on air substrate of thickness 'h' is shown in Fig. 1(a, b). The dimensions shown in figures and their captions are in cm. For the desired resonance frequency, patch length 'L' is calculated by using resonance frequency equation for RMSA as given in equation (1) [1 – 3].

$$f_r = \frac{c}{2\sqrt{\varepsilon_{re}}}\sqrt{\left(\frac{m}{L_e}\right)+\left(\frac{n}{W_e}\right)} \quad (1)$$

Where, f_r = RMSA resonance frequency (in Hz)
$c = 3 \times 10^8$ (m/s), velocity of light in free space
L_e = effective patch length, W_e = effective patch width, they include an extension in patch dimensions due to fringing fields towards open circuit patch edges (in cm)
m and n: mode indices, m = 1 and n = 0 for TM_{10} mode
ε_{re} = effective dielectric constant = 1, for air substrate

$$W_e = 1.2\ L_e \quad (2)$$

Using the above value of 'L_e' and 'W_e', the RMSA is simulated and the resonance frequency is noted from the resonance curve plot. If this value does not coincide with desired frequency then RMSA side length is further altered. After every variation in patch length, patch width is modified such that relation in equation (2) is maintained. Further the simulation is carried out until the peak in resonance curve matches the desired frequency value. For this frequency, value of patch side length 'L_e' is noted and fringing field extension length (Δl) is calculated by using equation (3).

$$\Delta l = \frac{\left(\frac{\lambda_0}{2} - L_e\right)}{2} \tag{3}$$

At fundamental TM_{10} mode, the patch is half wavelength resonator and therefore patch length 'L_e' is subtracted from half the wavelength. Since the fringing field extension is present towards both the open circuit patch edges, the difference value is divided by two. The above procedure is repeated for different values of 'h' and at different frequencies in 500 to 6000 MHz range and 'Δl' is calculated. Further to realize neural network model, the above data sets of the values of resonance frequency, substrate thickness, fringing field extension length and the air dielectric constant are used as discussed below.

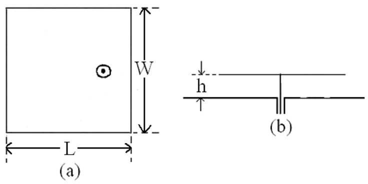

Fig. 1 (a) Top and (b) side views of coaxially fed RMSA

3. ANN MODEL FOR RMSA

The feed-forward standard back-propagation algorithm is used as a neural network model for RMSA. This is a supervised neural network model. The neural network model for RMSA is shown in Fig. 2(a, b). The supervised network is trained using input data and target data. The neural network learns from the input data and transforms input data into a desired response with the help of target data. They can approximate virtually any input-output map. They have been shown to approximate the performance of optimal statistical classifiers in difficult problems. The basic MLP (multi-level perceptron) building unit is a simple model of artificial neurons. This unit computes the weighted sum of the inputs plus the threshold weight and passes this sum through the activation function. In a multi-layer perceptron, the outputs of the units in one layer forms the inputs to the next layer. The weights of the network are usually computed by training the network using the back propagation algorithm. The supervised network, which has a configuration of 4 input neurons, 10 hidden neurons in a hidden layer and 1 output neurons which is trained for 50 epochs. The ANN model is trained with 6 samples and tested with the samples which fall under $0.1\lambda_0$ samples determined according to the definition of the problem. The parameters fed to the input of ANN are substrate thickness, fringing field extension length, dielectric constant at different resonant frequencies. The patch side length at different resonant frequencies and for different substrate thickness is predicted at the output of a trained neural network. For the predicted value, RMSA is simulated using IE3D software and the resonance frequency in its resonance curve is noted. The % error between the simulated and actual desired value (as given by ANN model) is calculated. The results obtained using ANN model for different frequencies and substrate thickness are tabulated in Table 1 to 20. They show close matching with simulated frequencies. The measurements were carried out at each frequency points as given in respective tables. In measurements the patch is fabricated using copper plate and it was suspended in air using foam spacer support placed towards the antenna corners. The foam spacer has dielectric constant close to unity, hence it does not affect the overall dielectric constant of the antenna. The measurement was carried out using R & S VNA (ZVH 8). Further similar ANN model is developed for suspended RMSA in which patch is fabricated on glass epoxy substrate which is suspended above the ground plane with an air gap 'Δ' as shown in Fig. 3(a, b). In this case an effective dielectric constant is calculated by using the effective dielectric constant formulae for two capacitors connected in parallel. In this case also the ANN model gives close prediction with simulated and measured results. Thus the proposed model can be used to design RMSA on suspended thicker substrate over wide frequency range.

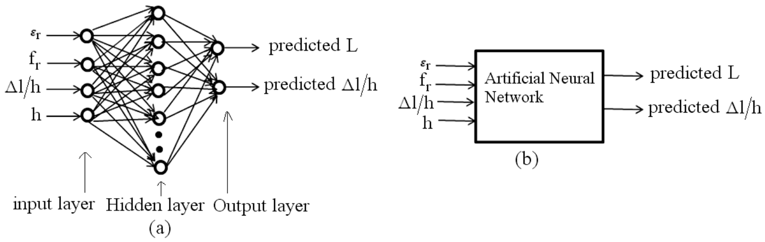

Fig. 2 (a, b) Artificial Neural Network model for coaxially fed suspended RMSA

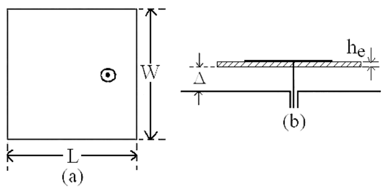

Fig. 3 (a, b) Co-axially fed RMSA fabricated on suspended glass epoxy substrate

Table 1 - Comparison between simulated, predicted and measured results around 500 MHz

h (cm)	h/λ_o	f_{ie3d} (MHz)	f_{ANN} (MHz)	$f_{measured}$ (MHz)	% Error
1	0.016	494.7	500	484.81	1.06
2	0.033	486.58	500	476.85	2.684
3	0.05	483.04	500	473.38	3.392
4	0.066	482.53	500	472.88	3.494
5	0.083	488.1	500	478.34	2.38
6	0.1	498.73	500	488.76	0.284

Table 2 - Comparison between simulated, predicted and measured results around 700 MHz

h (cm)	h/λ_o	f_{ie3d} (MHz)	f_{ANN} (MHz)	$f_{measured}$ (MHz)	% Error
0.5	0.011	693.291	700	679.43	0.96
1	0.023	694.05	700	680.15	0.85
1.5	0.035	685.32	700	671.61	2.097
2	0.047	683.04	700	669.38	2.42
2.5	0.058	684.94	700	671.24	2.15
3	0.07	689.114	700	675.33	1.55
3.5	0.082	697.85	700	683.89	0.31
4	0.093	709.24	700	695.6	1.32

Table 3 - Comparison between simulated, predicted and measured results around 900 MHz

h (cm)	h/λ_o	f_{ie3d} (MHz)	f_{ANN} (MHz)	$f_{measured}$ (MHz)	% Error
0.5	0.015	892.53	900	874.68	0.83
1.0	0.03	897.5	900	879.55	0.28
1.5	0.045	903.17	900	885.11	0.35
2.0	0.06	905.1	900	886.99	0.57
2.7	0.081	917.59	900	899.24	1.95
3	0.09	881.14	900	863.52	2.1

Table 4 - Comparison between simulated, predicted and measured results at around 1000 MHz

h (cm)	h/λ_o	f_{ie3d} (MHz)	f_{ANN} (MHz)	$f_{measured}$ (MHz)	% Error
0.1	0.0033	989.9	1000	970.1	1.01
0.3	0.01	981.8	1000	962.16	1.82
0.5	0.016	973.7	1000	954.23	2.63
0.7	0.023	971.65	1000	952.28	2.84
0.9	0.03	994.94	1000	975.04	0.51
1	0.033	987.2	1000	967.46	1.28

Table 5 - Comparison between simulated, predicted and measured results at around 1200 MHz

h (cm)	h/λ_o	f_{ie3d} (MHz)	f_{ANN} (MHz)	$f_{measured}$ (MHz)	% Error
0.4	0.016	1189	1200	1165.22	0.92
0.8	0.032	1206	1200	1181.9	0.5
1.6	0.064	1168	1200	1144.64	2.67
2	0.08	1180	1200	1156.4	1.67
2.4	0.096	1231	1200	1206.4	2.58

Table 6 - Comparison between simulated, predicted and measured results at around 1400 MHz

h (cm)	h/λ_o	f_{ie3d} (MHz)	f_{ANN} (MHz)	$f_{measured}$ (MHz)	% Error
0.4	0.018	1403	1400	1375	0.21
0.8	0.037	1413	1400	1385	0.93
1.2	0.056	1437	1400	1408.3	2.64
1.6	0.074	1362	1400	1334.8	2.71
2	0.093	1352	1400	1324.96	3.43

Table 7- Comparison between simulated, predicted and measured results at around 1800 MHz

h (cm)	h/λ_o	f_{ie3d} (MHz)	f_{ANN} (MHz)	$f_{measured}$ (MHz)	% Error
0.1	0.006	1777	1800	1741.5	1.28
0.3	0.018	1767	1800	1731.7	1.833
0.5	0.03	1798	1800	1762.04	0.11
0.9	0.054	1791	1800	1755.2	0.5
1.1	0.066	1816	1800	1779.7	0.89

Table 8- Comparison between simulated, predicted and measured results at around 2000 MHz

h (cm)	h/λ_o	f_{ie3d} (MHz)	f_{ANN} (MHz)	$f_{measured}$ (MHz)	% Error

0.1	0.0066	2007	2000	1966.86	0.35
0.2	0.013	2022	2000	1981.56	1.1
0.3	0.02	2057	2000	2015.86	2.85
0.4	0.027	2067	2000	2025.66	3.4
0.6	0.04	2033	2000	1992.34	1.7
1.2	0.08	2011	2000	1970.78	0.55

Table 9 - Comparison between simulated, predicted and measured results at around 2200 MHz

h (cm)	h/λ_o	f_{ie3d} (MHz)	f_{ANN} (MHz)	$f_{measured}$ (MHz)	% Error
0.1	0.0073	2172	2200	2128.56	1.27
0.2	0.014	2166	2200	2122.7	1.55
0.4	0.029	2203	2200	2158.9	0.14
0.5	0.037	2250	2200	2205	2.23
0.6	0.044	2275	2200	2229.5	3.41

Table 10 - Comparison between simulated, predicted and measured results at around 2400 MHz

h (cm)	h/λ_o	f_{ie3d} (MHz)	f_{ANN} (MHz)	$f_{measured}$ (MHz)	% Error
0.1	0.008	2373	2400	2325.54	1.13
0.2	0.016	2373	2400	2325.54	1.13
0.3	0.024	2380	2400	2332.4	0.833
0.4	0.032	2398	2400	2350	0.0833
0.5	0.04	2440	2400	2391.2	1.67

Table 11 - Comparison between simulated, predicted and measured results at around 2600 MHz

h (cm)	h/λ_o	f_{ie3d} (MHz)	f_{ANN} (MHz)	$f_{measured}$ (MHz)	% Error
0.1	0.0087	2575	2600	2523.5	0.96
0.2	0.017	2585	2600	2533.3	0.58
0.3	0.025	2608	2600	2555.8	0.31
0.4	0.034	2635	2600	2582.3	1.35
0.5	0.043	2656	2600	2602.9	2.15
0.8	0.07	2618	2600	2565.6	0.69
1.2	0.103	2638	2600	2585.2	1.46

Table 12 - Comparison between simulated, predicted and measured results at around 2800 MHz

h (cm)	h/λ_o	f_{ie3d} (MHz)	f_{ANN} (MHz)	$f_{measured}$ (MHz)	% Error
0.1	0.0093	2780	2800	2724.4	0.71
0.2	0.019	2785	2800	2729.3	0.54
0.3	0.028	2810	2800	2753.8	0.36
0.4	0.037	2901	2800	2842.98	3.61

Table 13 - Comparison between simulated, predicted and measured results at around 3000 MHz

h (cm)	h/λ_o	f_{ie3d} (MHz)	f_{ANN} (MHz)	$f_{measured}$ (MHz)	% Error

0.1	0.01	2996	3000	2936.1	0.133
0.2	0.02	3006	3000	2945.9	0.2
0.3	0.03	2976	3000	2916.5	0.8
0.4	0.04	3020	3000	2959.6	0.67
0.6	0.06	2930	3000	2871.4	2.33

Table 14 - Comparison between simulated, predicted and measured results at around 3400 MHz

h (cm)	h/λ_o	f_{ie3d} (MHz)	f_{ANN} (MHz)	$f_{measured}$ (MHz)	% Error
0.1	0.011	3304	3400	3237.9	2.82
0.2	0.022	3312	3400	3245.8	2.59
0.3	0.034	3424	3400	3355.5	0.71
0.4	0.045	3500	3400	3430	2.94
0.6	0.068	3356	3400	3426	1.29

Table 15 - Comparison between simulated, predicted and measured results at around 3500 MHz

h (cm)	h/λ_o	f_{ie3d} (MHz)	f_{ANN} (MHz)	$f_{measured}$ (MHz)	% Error
0.1	0.011	3445	3500	3376.1	1.57
0.2	0.023	3437	3500	3403.5	1.8
0.3	0.035	3455	3500	3385.9	1.29
0.4	0.047	3483	3500	3413.3	0.49

Table 16 - Comparison between simulated, predicted and measured results at around 4000 MHz

h (cm)	h/λ_o	f_{ie3d} (MHz)	f_{ANN} (MHz)	$f_{measured}$ (MHz)	% Error
0.1	0.0133	3936	4000	3857.3	1.6
0.2	0.027	3936	4000	3857.3	1.6
0.3	0.04	3980	4000	3900.4	0.5
0.4	0.053	4036	4000	3955.3	0.9
0.8	0.11	4178	4000	4094.4	4.45

Table 17 - Comparison between simulated, predicted and measured results at around 4500 MHz

h (cm)	h/λ_o	f_{ie3d} (MHz)	f_{ANN} (MHz)	$f_{measured}$ (MHz)	% Error
0.1	0.015	4384	4500	4296.3	2.58
0.2	0.03	4347	4500	4260.1	3.4
0.3	0.045	4414	4500	4325.7	1.91
0.4	0.06	4527	4500	4436.5	0.6

Table 18 - Comparison between simulated, predicted and measured results at around 5000 MHz

h (cm)	h/λ_o	f_{ie3d} (MHz)	f_{ANN} (MHz)	$f_{measured}$ (MHz)	% Error
0.1	0.017	4986	5000	4886.3	0.28
0.2	0.033	5087	5000	4985.3	1.74
0.3	0.05	5220	5000	5115.6	4.4
0.4	0.067	4980	5000	4880	0.4

Table 19 - Comparison between simulated, predicted and measured results at around 5500 MHz

h (cm)	h/λ_o	f_{ie3d} (MHz)	f_{ANN} (MHz)	$f_{measured}$ (MHz)	% Error

0.1	0.018	5544	5500	5433.1	0.8
0.2	0.037	5512	5500	5401.8	0.22
0.3	0.055	5586	5500	5474.3	1.56
0.4	0.073	5504	5500	5393.9	0.073

Table 20 - Comparison between simulated, predicted and measured results at around 6000 MHz

h (cm)	h/λ_o	f_{ie3d} (MHz)	f_{ANN} (MHz)	$f_{measured}$ (MHz)	% Error
0.1	0.02	6070	6000	5948.6	1.17
0.3	0.06	6138	6000	6015.24	2.3
0.4	0.08	5868	6000	5751	2.2

4. CONCLUSIONS

The Artificial neural network model for suspended RMSA over a wide frequency range and varying substrate thickness is proposed. The neural network model was developed using parameters like, substrate thickness, dielectric constant, resonance frequency and an edge extension length in terms of substrate thickness. The predicted patch side length was obtained from the neural network which when simulated using IE3D software gives closer match with the desired patch resonance frequency. Further the measurements were carried out to validate the simulated results. The measured results are in close agreement with predicted and simulated values. The similar model is developed for suspended RMSA in which the radiating patch is fabricated on suspended glass epoxy substrate. In this case also closer agreement between simulated, predicted and measured results is obtained. Thus the proposed model can be used to design RMSA on thicker substrate and at any given frequency. In the world of miniaturization, compact MSAs are widely used. The closer form expressions to calculate shorted patch length in compact MSAs is not available. In the future work, similar neural network model will be developed to accurately calculate the edge extension length / shorted patch length in compact MSAs.

References

[1] Wong, K. L., 2002. Compact and Broadband Microstrip Antennas, 1st edn., John Wiley & sons, Inc., New York, USA.
[2] Garg, R., Bhartia, P., Bahl, I., Ittipiboon, A., 2001. Microstrip Antenna Design Handbook, Artech House, USA.
[3] Kumar, G., Ray, K. P., 2003. Broadband Microstrip Antennas, 1st edn., Artech House, USA.
[4] Kushwah, V. S., Tomar, G. S., 2009. Design of Microstrip Patch Antennas Using Neural Network, Proceedings of Third Asia International Conference on Modelling & Simulation, Bali, (DOI - 10.1109/AMS.2009.12).
[5] Turker, N., Gunes, F., Yildirim, T., 2006. Artificial Neural Design of Microstrip Antennas, Turk J Elec Engin, 14, 3, 445 – 453.
[6] IE3D 12.1, Zeland Software, Freemont, USA, 2004.